

Figure 8.29 (a) Tank using lossy varactor, (b) equivalent circuit.

$R_{var}$  to a parallel combination [Fig. 8.29(b)], we have from Chapter 2

$$R_{p2} = \frac{1}{C_{var}^2 \omega^2 R_{var}}. \quad (8.60)$$

To utilize our previous results, we combine  $C_1$  and  $C_{var}$ . The  $Q$  associated with  $C_1 + C_{var}$  is equal to

$$Q_C = R_{p2}(C_1 + C_{var})\omega \quad (8.61)$$

$$= \frac{C_1 + C_{var}}{C_{var}^2 \omega R_{var}}. \quad (8.62)$$

Recognizing that  $Q_{var} = (C_{var}\omega R_{var})^{-1}$ , we have

$$Q_C = \left(1 + \frac{C_1}{C_{var}}\right) Q_{var}. \quad (8.63)$$

In other words, the  $Q$  of the varactor is “boosted” by a factor of  $1 + C_1/C_{var}$ . The overall tank  $Q$  is therefore given by

$$\frac{1}{Q_{tot}} = \frac{1}{Q_L} + \frac{1}{\left(1 + \frac{C_1}{C_{var}}\right) Q_{var}}. \quad (8.64)$$

For frequencies as high as several tens of gigahertz, the first term in Eq. (8.64) is dominant (unless a long channel is chosen for the varactors).

Equation (8.64) can be generalized if the tank consists of an ideal capacitor,  $C_1$ , and lossy capacitors,  $C_2$ – $C_n$ , that exhibit a series resistance of  $R_2$ – $R_n$ , respectively. The reader can prove that

$$\frac{1}{Q_{tot}} = \frac{1}{Q_L} + \frac{C_2}{C_{tot}} \frac{1}{Q_2} + \dots + \frac{C_n}{C_{tot}} \frac{1}{Q_n}, \quad (8.65)$$

where  $C_{tot} = C_1 + \dots + C_n$  and  $Q_j = (R_j C_j \omega)^{-1}$ .

## 8.6 LC VCOs WITH WIDE TUNING RANGE

### 8.6.1 VCOs with Continuous Tuning

The tuning range obtained from the C–V characteristic depicted in Fig. 8.27 may prove prohibitively narrow, particularly because the capacitance range corresponding to *negative*

$V_{GS}$  (for  $V_{cont} > V_{DD}$ ) remains unused. We must therefore seek oscillator topologies that allow both positive and negative (average) voltages across the varactors, utilizing almost the entire range from  $C_{min}$  to  $C_{max}$ .

Figure 8.30(a) shows one such topology. Unlike the tail-biased configuration studied in Section 8.3, this circuit defines the bias currents of  $M_1$  and  $M_2$  by a *top* current source,  $I_{DD}$ . We analyze this circuit by first computing the output common-mode level. In the absence of oscillation, the circuit reduces to that shown in Fig. 8.30(b), where  $M_1$  and  $M_2$  share  $I_{DD}$  equally and are configured as diode-connected devices. Thus, the CM level is simply given by the gate-source voltage of a diode-connected transistor carrying a current of  $I_{DD}/2$ .<sup>4</sup> For example, for square-law devices,

$$V_{GS1,2} = \sqrt{\frac{I_{DD}}{\mu_n C_{ox}(W/L)}} + V_{TH}. \quad (8.66)$$

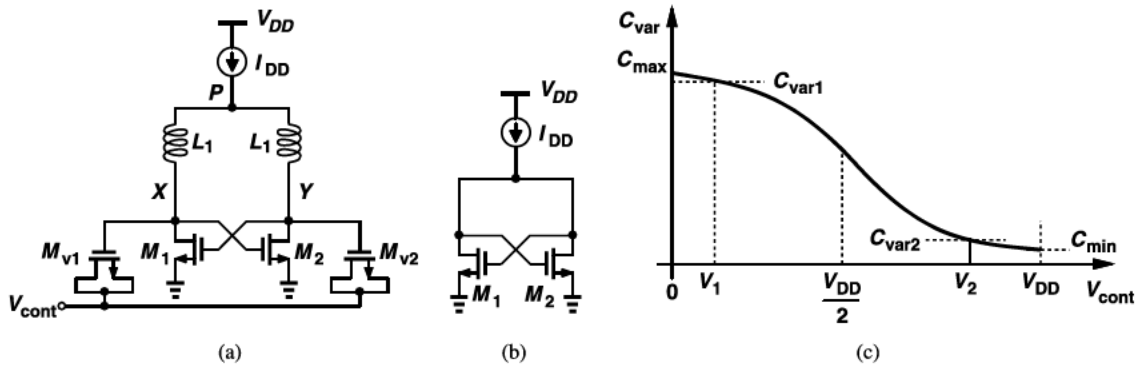


**Figure 8.30** (a) Top-biased VCO, (b) equivalent circuit for CM calculation, (c) varactor range used.

We select the transistor dimensions such that the CM level is approximately equal to  $V_{DD}/2$ . Consequently, as  $V_{cont}$  varies from 0 to  $V_{DD}$ , the gate-source voltage of the varactors,  $V_{GS,var}$ , goes from  $+V_{DD}/2$  to  $-V_{DD}/2$ , sweeping almost the entire capacitance range from  $C_{min}$  to  $C_{max}$  [Fig. 8.30(c)]. In practice, the circuit producing  $V_{cont}$  (the charge pump) can handle only the voltage range from  $V_1$  to  $V_2$ , yielding a capacitance range from  $C_{var1}$  to  $C_{var2}$ .

The startup condition, oscillation frequency, and output swing of the oscillator shown in Fig. 8.30(a) are similar to those derived for the tail-biased circuit of Fig. 8.18(b). Also,  $L_1$  and  $L_2$  are realized as a single symmetric inductor so as to achieve a higher  $Q$ ; the center tap of the inductor is tied to  $I_{DD}$ .

While providing a wider range than its tail-biased counterpart, the topology of Fig. 8.30(a) suffers from a higher phase noise. As studied in Section 8.7, this penalty arises primarily from the modulation of the output CM level (and hence the varactors) by the noise current of  $I_{DD}$ , as evidenced by Eq. (8.66). This effect does not occur in the tail-biased oscillator because the output CM level is “pinned” at  $V_{DD}$  by the low dc resistance of the inductors. The following example illustrates this difference.

4. With large-signal oscillation, the nonlinearity of  $M_1$  and  $M_2$  shifts the output CM level slightly, but we neglect this effect here.

**Example 8.16**

The tail or top bias current in the above oscillators is changed by  $\Delta I$ . Determine the change in the voltage across the varactors.

**Solution:**

As shown in the tail-biased topology of Fig. 8.31(a), each inductor contains a small low-frequency resistance,  $r_s$  (typically no more than  $10\ \Omega$ ). If  $I_{SS}$  changes by  $\Delta I$ , the output CM level changes by  $\Delta V_{CM} = (\Delta I/2)r_s$ , and so does the voltage across each varactor. In the top-biased circuit of Fig. 8.31(b), on the other hand, a change of  $\Delta I$  flows through two diode-connected transistors, producing an output CM change of  $\Delta V_{CM} = (\Delta I/2)(1/g_m)$ . Since  $1/g_m$  is typically in the range of a few hundred ohms, the top-biased topology suffers from a much higher varactor voltage modulation.

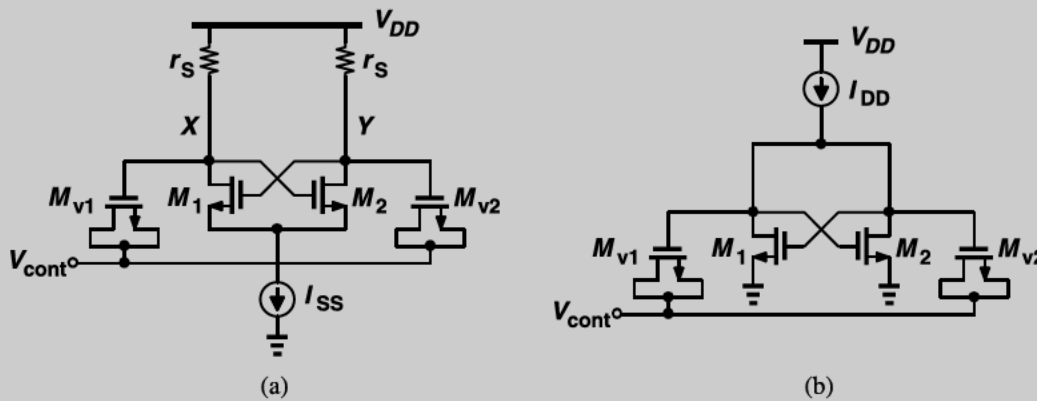


**Figure 8.31** Output CM dependence on bias current in (a) tail-biased and (b) top-biased VCOs.

**Example 8.17**

What is the change in the oscillation frequency in the above example?

**Solution:**

Since a CM change at X and Y is indistinguishable from a change in  $V_{cont}$ , we have

$$\Delta\omega = K_{VCO}\Delta V_{CM} \quad (8.67)$$

$$= K_{VCO}\frac{\Delta I}{2}r_s \quad \text{or} \quad K_{VCO}\frac{\Delta I}{2}\frac{1}{g_m}. \quad (8.68)$$

In order to avoid varactor modulation due to the noise of the bias current source, we return to the tail-biased topology but employ *ac coupling* between the varactors and the core so as to allow positive and negative voltages across the varactors. Illustrated in Fig. 8.32(a),

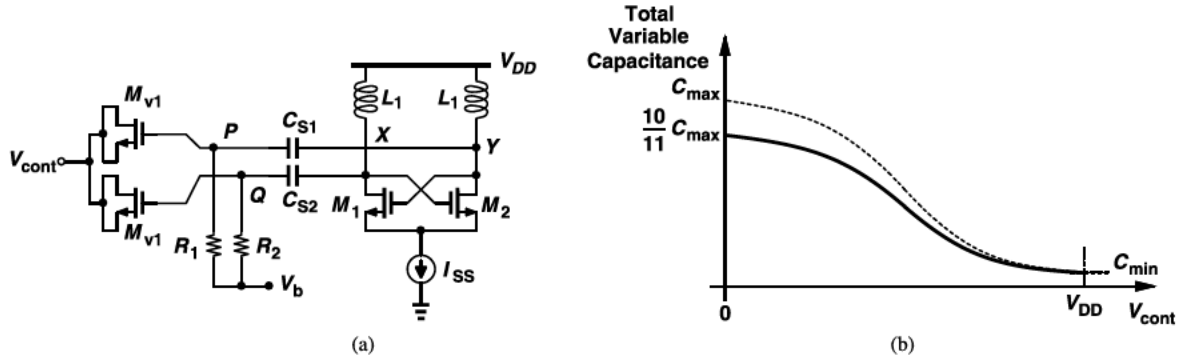


**Figure 8.32** (a) VCO using capacitor coupling to varactors, (b) reduction of tuning range as a result of finite  $C_{S1}$  and  $C_{S2}$ .

the idea is to define the dc voltage at the gate of the varactors by  $V_b$  ( $\approx V_{DD}/2$ ) rather than  $V_{DD}$ . Thus, in a manner similar to that shown in Fig. 8.30(c), the voltage across each varactor goes from  $-V_{DD}/2$  to  $+V_{DD}/2$  as  $V_{cont}$  varies from 0 to  $V_{DD}$ , maximizing the tuning range.

The principal drawback of the above circuit stems from the parasitics of the coupling capacitors. In Fig. 8.32(a),  $C_{S1}$  and  $C_{S2}$  must be *much greater* than the maximum capacitance of the varactors,  $C_{max}$ , so that the capacitance range presented by the varactors to the tanks does not shrink substantially. If  $C_{S1} = C_{S2} = C_S$ , then in Eq. (8.53),  $C_{var2}$  and  $C_{var1}$  must be placed in series with  $C_S$ , yielding

$$\Delta\omega_{os} \approx \frac{1}{\sqrt{L_1 C_1}} \cdot \frac{1}{2C_1} \cdot \frac{C_S^2 (C_{var2} - C_{var1})}{(C_S + C_{var2})(C_S + C_{var1})}. \quad (8.69)$$

For example, if  $C_S = 10C_{max}$ , then the series combination yields a maximum capacitance of  $(10C_{max} \cdot C_{max})/(11C_{max}) = (10/11)C_{max}$ , i.e., about 10% less than  $C_{max}$ . Thus, as shown in Fig. 8.32(b), the capacitance range decreases by about 10%. Equivalently, the maximum-to-minimum capacitance ratio falls from  $C_{max}/C_{min}$  to  $(10C_{max} + C_{min})/(11C_{min}) \approx (10/11)(C_{max}/C_{min})$ .